This journal is © The Royal Society of Chemistry 2010

Supporting Information for "Incorporation of the Dopamine D2L receptor and bacteriorhodopsin within bicontinuous cubic lipid phases. 1. Relevance to *in meso* crystallization of integral membrane proteins in monoolein systems"

(1) Representative 1-D diffraction plots

In all images the (hkl) reflections corresponding to the particular lipid mesophase adopted are highlighted. Peaks corresponding to a Q_{II}^{D} cubic phase are indicated in normal type, peaks corresponding to a Q_{II}^{G} cubic phase in bold type and peaks corresponding to a H_{II} phase in italic type. For some plots the intensity has been plotted on a logarithmic scale to visualize less intense peaks.

Incorporation of dopamine D2L receptor within MO (Batch 1)

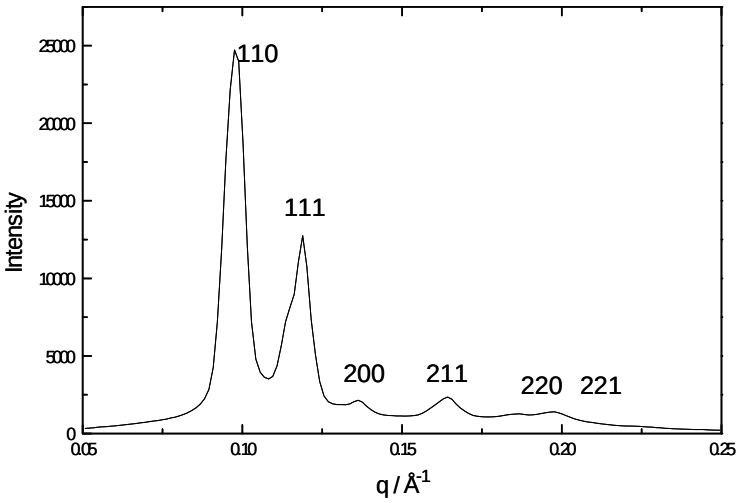

Figure S1. 1D diffraction pattern for MO 40wt% D2L receptor buffer (Batch 1). T=20°C. Peaks corresponding to a Q_{II}^{D} phase are observed. This corresponds to Fig. 4(A) but with the intensity plotted on a non-logarithmic scale.

This journal is © The Royal Society of Chemistry 2010

Incorporation of dopamine D2L **receptor within MO (Batch 2)**

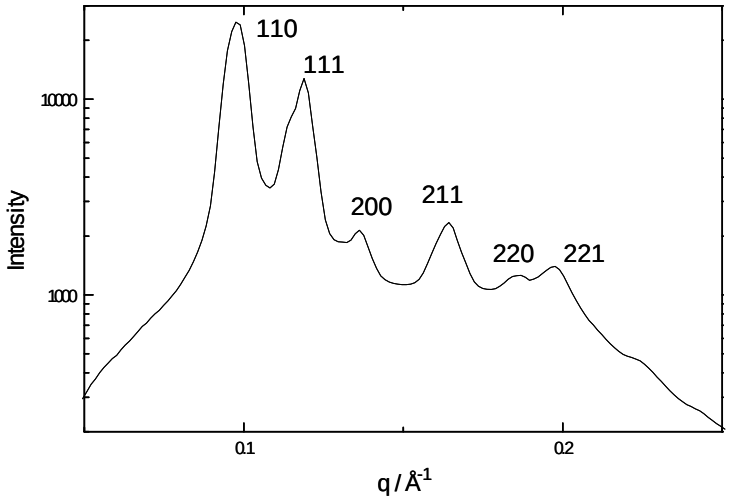

Figure S2. 1D diffraction pattern for MO 40wt% D2L receptor buffer (Batch 2). T=20°C. Peaks corresponding to a Q_{II}^{D} phase are observed.

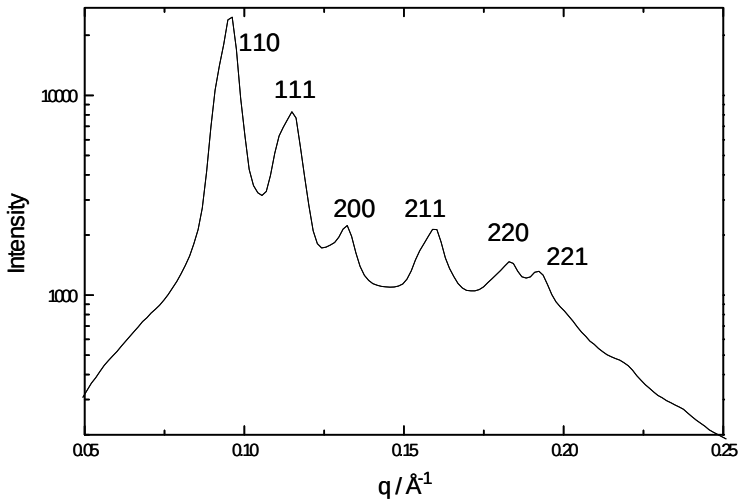

Figure S3. 1D diffraction pattern for MO 40wt% D2L receptor (Batch 2) at 0.55 mgs/ml. T=20°C. Peaks corresponding to a Q_{II}^{D} phase are observed.

This journal is © The Royal Society of Chemistry 2010

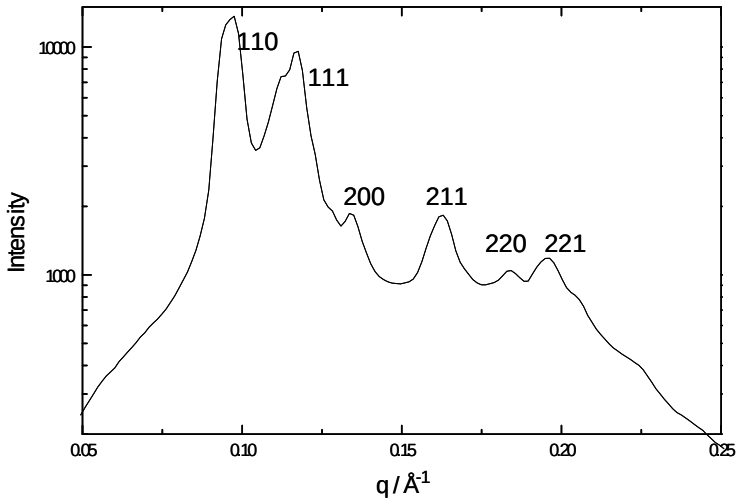

Figure S4. 1D diffraction pattern for MO 40wt% D2L receptor (Batch 2) at 1.1 mgs/ml. T=20°C. Peaks corresponding to a Q_{II}^{D} phase are observed. A shoulder to the low angle side of the Q_{II}^{D} (111) peak may correspond to a growing (211) reflection from the Q_{II}^{G} phase seen below.

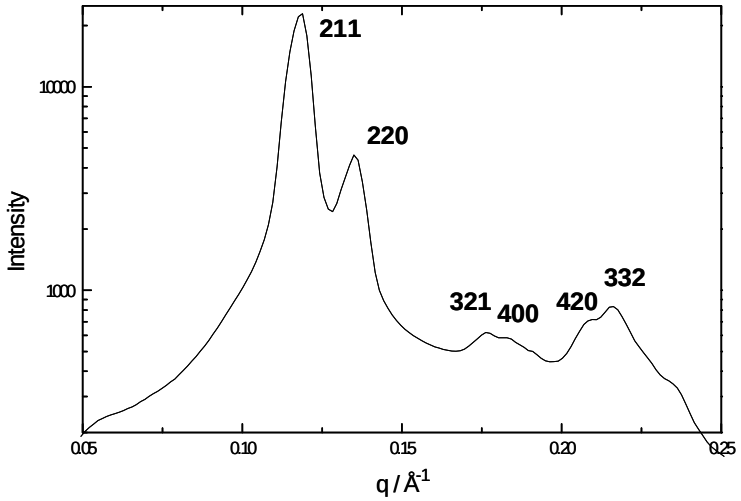

Figure S5. 1D diffraction pattern for MO 40wt% D2L receptor (Batch 2) at 2.2 mgs/ml. T=20°C. Peaks corresponding to a relatively weakly ordered Q_{II}^{G} phase are observed.

This journal is © The Royal Society of Chemistry 2010

Incorporation of bR within MO (Batch 1)

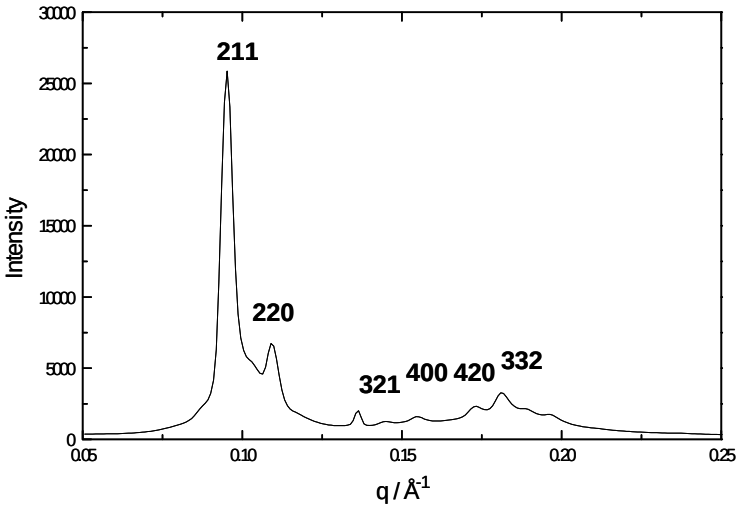

Figure S6. 1D diffraction pattern for MO 40wt% Na/K phosphate buffer (Batch 1). T=20°C. Peaks corresponding to a Q_{II}^{G} phase are observed.

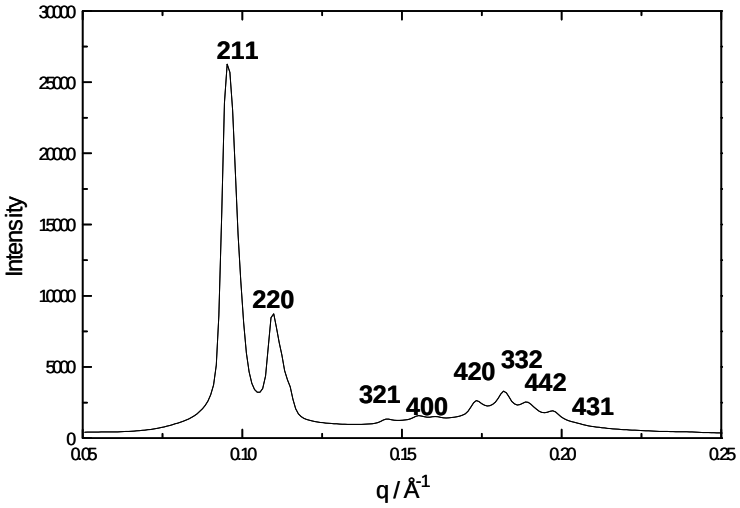

Figure S7. 1D diffraction pattern for MO 40wt% bR (Batch 1) at 1 mgs/ml. T=20°C. Peaks corresponding to a Q_{II}^{G} phase are observed.

This journal is © The Royal Society of Chemistry 2010

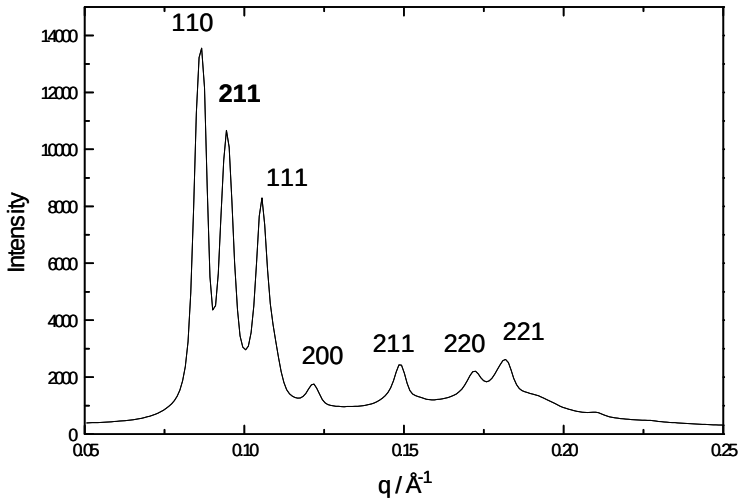

Figure S8. 1D diffraction pattern for MO 40wt% bR (Batch 1) at 6 mgs/ml. T=20°C. Peaks corresponding to a Q_{II}^{D} phase are observed along with a residual (211) peak from a Q_{II}^{G} phase.

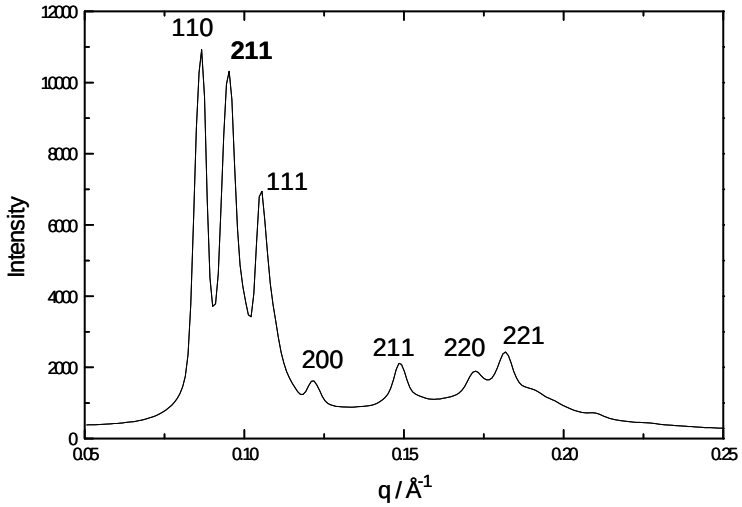

Figure S9. 1D diffraction pattern for MO 40wt% bR (Batch 1) at 9 mgs/ml. T=20°C. Peaks corresponding to a Q_{II}^{D} phase are observed along with a residual (211) peak from a Q_{II}^{G} phase.

This journal is © The Royal Society of Chemistry 2010

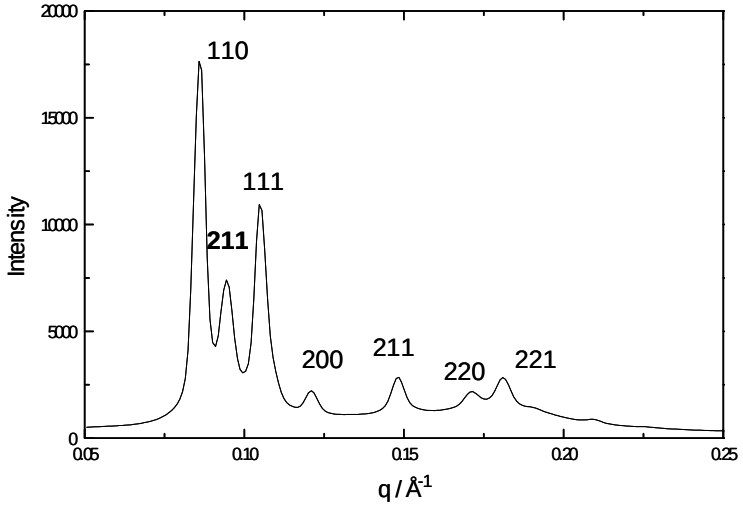

Figure S10. 1D diffraction pattern for MO 40wt% bR (Batch 1) at 18 mgs/ml. T=20°C. Peaks corresponding to a Q_{II}^{D} phase are observed along with a residual (211) peak from a Q_{II}^{G} phase.

Incorporation of bR within MO (Batch 2)

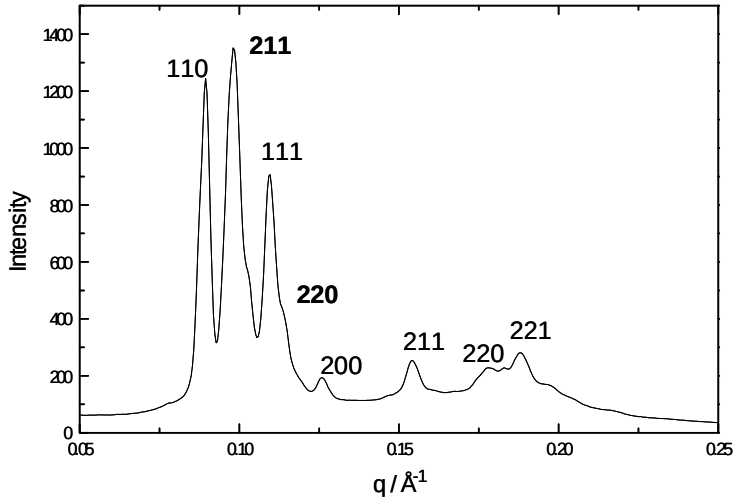

Figure S11. 1D diffraction pattern for MO 40wt% Na/K phosphate buffer (Batch 2). T=25°C. Peaks corresponding to co-existing Q_{II}^{D} and Q_{II}^{G} phases are observed

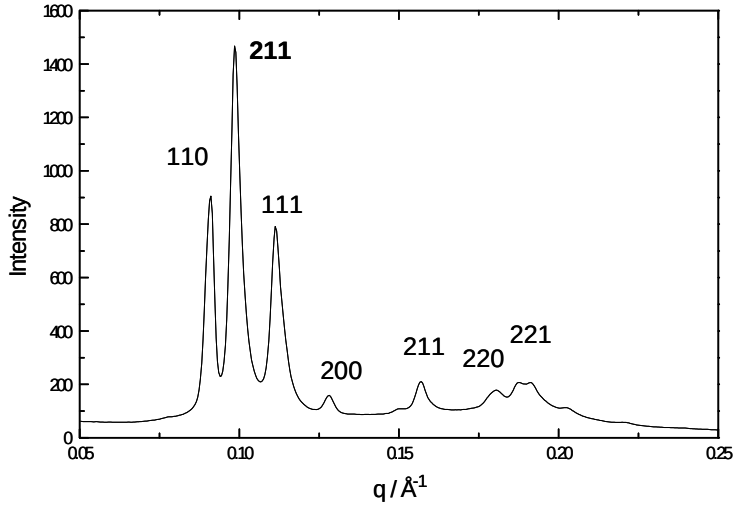

Figure S12. 1D diffraction pattern for MO 40wt% bR (Batch 2) at 3 mgs/ml. T=25°C. Peaks corresponding to co-existing Q_{II}^{D} and Q_{II}^{G} phases are observed**.**

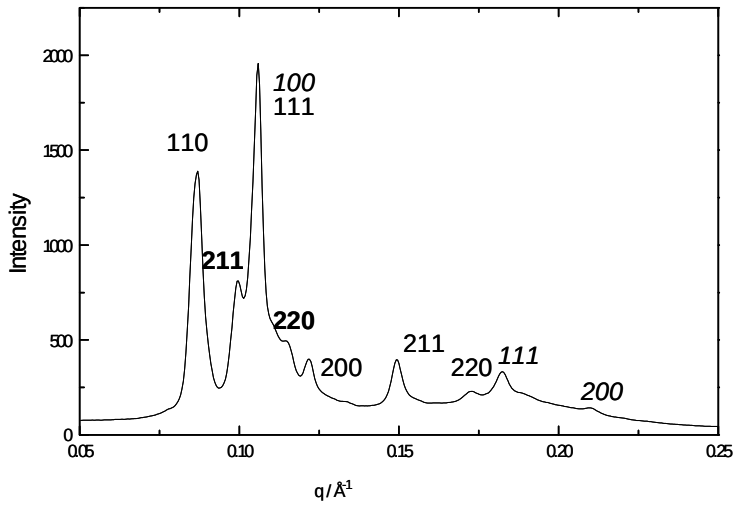

Figure S13. 1D diffraction pattern for MO 40wt% bR (Batch 2) at 18 mgs/ml. T=25°C. Co-existing Q_{II}^{D} and H_{II} phases are observed, along with weak residual peaks from a Q_{II}^{G} phase.

(2) Additional tables of lattice parameter, lipid length and water channel radius

[D2L] / mgs/ml	Cubic Phase	c / %	a / Å 20℃	Error / Å	a / Å 25℃	Error / Å	a / Å 30℃	Error / Å	a / Å 37℃	Error / Å
0	Q_{II}^{D}	41.4	98.1	0.1	97.3	0.1	95.2	0.1		
1.1	Q_{II}^{D}	41.4	100.6	0.1	99.5	0.1	96.2	0.1	90.4	0.1
2.2	Q_{II}^{D}	40.8	102.0	0.1	101.4	0.1	100.1	0.1	94.4	0.1
4.4	Q_{II}^{D}	41.6	100.4	0.1	99.1	0.1	96.1	0.1	93.4	0.2
4.4	Q_{II}^{G}	41.6	158.0		155.4		149.7		142.2	
6.6	Q_{II}^{G}	42.0	160.0	0.7	158.1	0.5	156.5	0.4	154.1	0.8
7.7	Q_{II}^{G}	42.1	167.4	0.7	165.8	0.8	163.5	1.3	160.8	1.6

Table S1. The phase adopted and lattice parameter of MO as a function of [D2L] and temperature for Batch 1 of the dopamine D2 receptor. This data is plotted in Figure 4 (A).

[bR] / mgs/ml	Cubic Phase	c / %	a / Å 20℃	Error / Å	a / Å 25℃	Error / Å	a / Å 30℃	Error / Å	a / Å 37℃	Error / Å
0	Q_{II}^{G}	39.9	162.8	0.4	161.5	0.8	160.9	0.5	147.4	0.9
	Q_{II}^{D}								93.8	0.4
1	Q_{II}^{G}	39.3	162.6	0.2	160.7	0.5	159.7	0.3	146.9	0.8
	Q_{II}^{D}								94.1	0.3
6	Q_{II}^{G}	38.9	163.3	0.1	161.2	-	158.2	-	155.3	-
	Q_{II}^{D}		103.7	0.1	101.9	0.6	99.7	0.4	97.3	0.3
9	Q_{II}^{G}	39.1	163.4	-	161.4	-	158.2	-	153.8	-
	Q_{II}^{D}		103.8	0.1	102.3	0.3	100.5	0.3	97.5	0.1
18	Q_{II}^{G}	39.7	164.3	-	162.8	-	159.5	-		
	Q_{II}^{D}		104.1	0.1	102.8	0.1	100.8	0.1	98.1	0.1

Table S2. The phase adopted and lattice parameter of MO as a function of [bR] and temperature for Batch 1 of bR. This data is plotted in Figure 4 (B).

[D2L] / mgs/ml	Phase	c / %	$ø_w$ / %	l / Å 21.3℃	r_w / Å 21.3℃	l / Å 25.0℃	r_w / Å 25.0℃	l / Å 28.8℃	r_w / Å 28.8℃
0	Q_{II}^D	40.2	37.9	17.2	21.5	17.0	21.3	17.0	21.3
0.55	Q_{II}^D	40.9	38.5	17.5	22.5	17.5	22.4	17.1	21.9
1.1	Q_{II}^D	40.1	37.8	17.4	21.8	17.3	21.7	17.1	21.4
2.2	Q_{II}^G	41.0	38.6	14.9	20.1	14.7	19.8	14.6	19.6

Table S3. The lipid length (l) and water channel radius (r_w) for MO in the presence of the dopamine D2 receptor (Batch 2). Data are presented as a function of protein concentration and temperature.

[bR] / mgs/ml	Phase	c / %	$ø_w$ / %	l / Å 21.3℃	r_w / Å 21.3℃	l / Å 25.0℃	r_w / Å 25.0℃	l / Å 28.7℃	r_w / Å 28.7℃
0	Q_{II}^D	40.9	38.5	17.7	22.7	17.4	21.8	17.2	21.6
	Q_{II}^G			17.0	22.8	16.9	22.2	16.7	22.0
3	Q_{II}^D	40.2	37.9	17.6	22.1	16.9	21.6	16.5	21.2
	Q_{II}^G			17.1	22.4	16.6	22.3	16.5	16.5
18	Q_{II}^D	40.2	37.9	18.1	22.8	17.9	22.5	17.7	17.7

Table S4. The lipid length (l) and water channel radius (r_w) for MO in the presence of bR (Batch 2). Data are presented as a function of protein concentration and temperature.

This journal is © The Royal Society of Chemistry 2010

(3) Background Scattering Analysis

The scattered intensity was fitted as a sum of the scattering from a diamond cubic phase and from bilayer sponge cell-cell correlations, in a similar manner to Angelov *et al*.[1]

Briefly the scattered intensity I(q) was plotted as a sum of the scattering from a bicontinuous cubic phase (see the scattering model in Refs.[2,3]) and from bilayer sponge cell-cell correlations.

Scattering from a cubic phase is given by Eq. S1

$$I(q) = \frac{c_1}{q^2} \sum_{hkl} \exp\left[-\frac{(q - q_{hkl})^2}{2\sigma^2} \right] I_{hkl} \qquad \text{(S1)}$$

$q=(2\pi/a)(h^2+k^2+l^2)^{1/2}$. The peak positions are given by q_{hkl}. The peak widths, σ, for the cubic phase peaks are assumed to be constant across all peaks. c_1 is an intensity normalization factor.

The individual peak intensities, I_{hkl} are given by Eq. S2

$$I_{hkl} = F_{hkl}^{\,S} \frac{2\rho_0}{\alpha_{hkl} q} \sin\left(\alpha_{hkl} q \frac{L}{2} \right) \qquad \text{(S2)}$$

The dimensionless structure factors F_{hkl}^{S*}, multiplicity factors M_{hkl} and α_{hkl} parameters for the gyroid and diamond surfaces are taken directly from Ref.[2]. ρ_0 is the electron density within the layer.

Scattering from bilayer sponge cell-cell correlations is given by Eq. S3

$$I(q) = \frac{c_2}{\xi^2 + (q - q_c)^2} \qquad \text{(S3)}$$

where q_c is the position of the diffuse sponge peak, ξ is the correlation length and c_2 is an intensity normalization factor.

This journal is © The Royal Society of Chemistry 2010

The scattered intensity from two representative 1D scattering patterns for MO 40wt% D2L at 1.1mgs/ml (Fig. S14) and MO 40wt% D2L buffer (Fig. S15) was fitted in this way. In both cases scattering from bilayer sponge cell-cell correlations appears to be a reasonable approximation to the diffuse scattering background consistent with the work of Angelov *et al*. We note that this holds both in the presence (Fig. S14) and absence (Fig. S15) of protein. In both cases the scattering did not approximate a Gaussian scattering pattern or the scattering from a micro-emulsion. As a thorough investigation is outside the scope of this research we therefore suggest that the scattering likely corresponds to regions of disorder within the cubic phase sample but are unable to comment definitively on the exact form of this scattering.

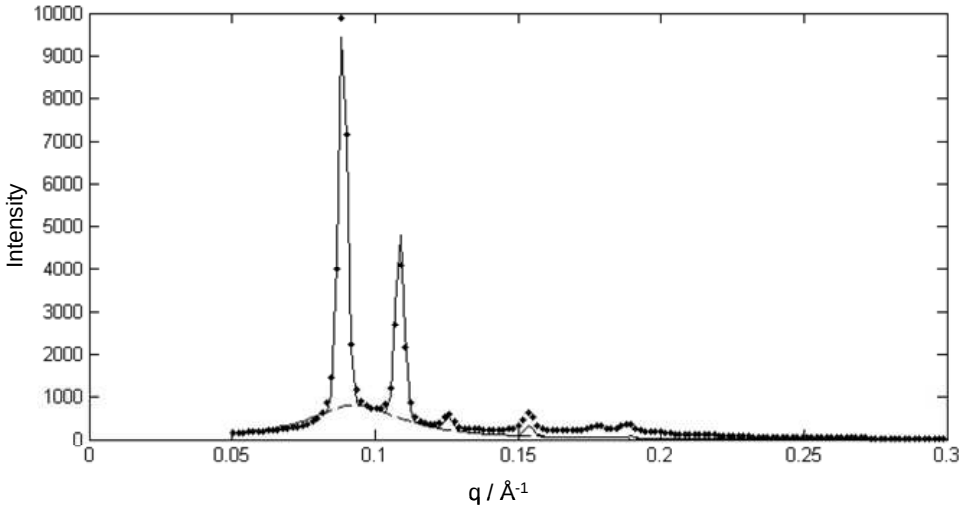

Figure S14. 1D diffraction pattern for MO 40wt% D2 (Batch 1) at 1.1 mgs/ml. The dashed line represents model scattering from bilayer sponge cell-cell correlations (Eq. S3).[1] The solid line is the resulting fit for the cubic phase and the sponge cell-cell correlations.

This journal is © The Royal Society of Chemistry 2010

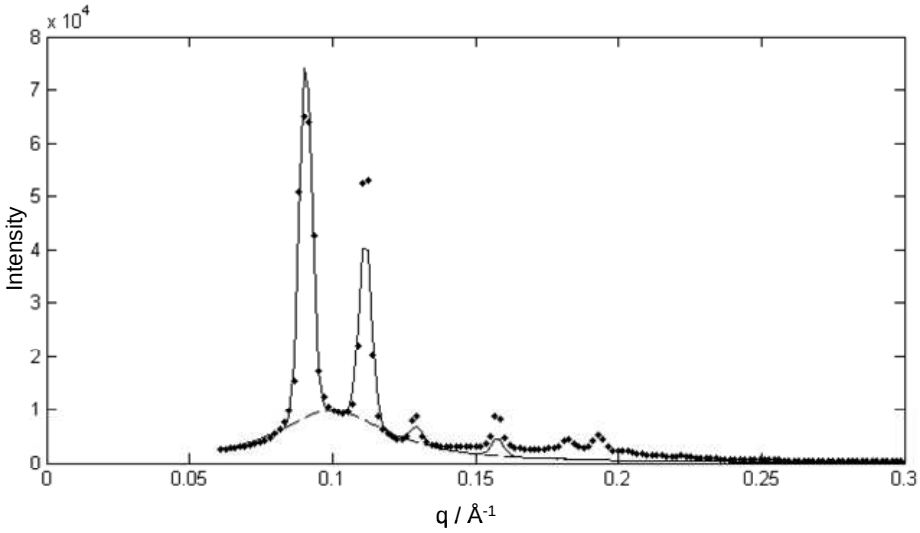

Figure S15. 1D diffraction pattern for MO 40wt% D2L buffer. The dashed line represents model scattering from bilayer sponge cell-cell correlations (Eq. S3).[1] The solid line is the resulting fit for the cubic phase and the sponge cell-cell correlations.

(1) Angelov, B.; Angelova, A.; Vainio, U.; Garamus, V. M.; Lesieur, S.; Willumeit, R.; Couvreur, P. *Langmuir* **2009**, *25*, 3734.
(2) Garstecki, P.; Holyst, R. *Langmuir* **2002**, *18*, 2519.
(3) Garstecki, P.; Holyst, R. *Langmuir* **2002**, *18*, 2529.